

Comprehensive imaging analysis of intracranial atherosclerosis

Sebastian Sanchez ¹, Mahmud Mossa-Basha ², Vania Anagnostakou ³,
David S Liebeskind,⁴ Edgar A Samaniego ⁵

► Additional supplemental material is published online only. To view, please visit the journal online (<https://doi.org/10.1136/jnis-2023-020622>).

¹Neurology, Yale University, New Haven, Connecticut, USA

²Radiology, University of Washington, Seattle, Washington, USA

³Radiology, University of Massachusetts Chan Medical School, Worcester, Massachusetts, USA

⁴Department of Neurology, University of California Los Angeles, Los Angeles, California, USA

⁵Neurology, Neurosurgery and Radiology, University of Iowa Hospitals and Clinics, Iowa City, Iowa, USA

Correspondence to

Dr Edgar A Samaniego, Neurology, Neurosurgery and Radiology, University of Iowa Hospitals and Clinics, Iowa City, Iowa, USA; edgarsama@gmail.com

Received 8 January 2024

Accepted 20 April 2024



© Author(s) (or their employer(s)) 2024. No commercial re-use. See rights and permissions. Published by BMJ.

To cite: Sanchez S, Mossa-Basha M, Anagnostakou V, et al. *J NeuroInterv Surg* Epub ahead of print: [please include Day Month Year]. doi:10.1136/jnis-2023-020622

ABSTRACT

Intracranial atherosclerotic disease (ICAD) involves the build-up of atherosclerotic plaques in cerebral arteries, significantly contributing to stroke worldwide. Diagnosing ICAD entails various techniques that measure arterial stenosis severity. Digital subtraction angiography, CT angiography, and magnetic resonance angiography are established methods for assessing stenosis. High-resolution MRI offers additional insights into plaque morphology including plaque burden, hemorrhage, remodeling, and contrast enhancement. These metrics and plaque traits help identify symptomatic plaques. Techniques like transcranial Doppler, CT perfusion, computational fluid dynamics, and quantitative MRA analyze blood flow restrictions due to ICAD. Intravascular ultrasound or optical coherence tomography have a very high spatial resolution and can assess the structure of the arterial wall and the plaque from the lumen of the target vascular territory. Positron emission tomography could further detect inflammation markers. This review aims to provide a comprehensive overview of the spectrum of current modalities for atherosclerotic plaque analysis and risk stratification.

INTRODUCTION

Intracranial atherosclerotic disease (ICAD) comprises atherosclerotic changes within the intracranial portion of the vasculature supplying the brain. This condition stands as a prevalent contributor to ischemic stroke and transient ischemic attacks, posing a substantial health challenge on a global scale.¹ Studies estimate that 20–40 individuals per 100 000 worldwide suffer cerebral infarctions associated with ICAD.² Various efforts to characterize the vascular changes of intracranial disease have led to the description of multiple characteristics of high-risk intracranial plaques such as degree of luminal stenosis, absence of collateral flow, plaque ulceration, plaque burden (PB), intraplaque hemorrhage (IPH), and plaque enhancement after the administration of contrast gadolinium (Gd).³ Currently, there are various imaging modalities and techniques used to assess the extent and burden of atherosclerotic changes (table 1). This review aims to provide a summary of the diverse imaging modalities and methods of analyzing and characterizing intracranial atherosclerotic changes.

Digital subtraction angiography (DSA) is a luminal imaging modality in which the interventionalist navigates a catheter through the vasculature. It is the gold standard for the diagnosis of luminal

stenosis and provides unique real-time hemodynamic information. CT angiography (CTA) uses radiation to assess the brain vasculature. It provides accurate information about the arterial lumen and can identify components of the plaque. MR angiography (MRA) is a luminal modality that does not use radiation. It provides an accurate representation of the arterial lumen, but it cannot visualize the plaque components unless it is accompanied by a high-resolution MRI (HR-MRI) protocol. HR-MRI provides information about the arterial wall and the plaque. Transcranial ultrasound assesses the flow velocity to obtain indirect measurements of stenosis. It can provide hemodynamic information, but it does not assess the plaque's characteristics. Intravascular ultrasound (IVUS) is a modality in which an ultrasound probe is navigated through the vasculature. It provides a very high spatial resolution due to proximity with the plaque; however, it remains an invasive modality. Optical coherence tomography (OCT) uses an intravascular probe to directly assess the plaque. Although it is an invasive imaging modality, it has very good correlation with the plaque components.

DETERMINATION OF DEGREE OF STENOSIS

Luminal stenosis plays a crucial role in assessing the risk profiles of atherosclerotic plaque. It refers to the narrowing or constriction of the arterial lumen caused by plaque formation. Stenosis is generally quantified by comparing the diameter or cross-sectional area of the constricted segment with that of a normal reference segment in the same artery.⁴ The widely used Warfarin-Aspirin Symptomatic Intracranial Disease (WASID) criteria categorize stenosis into four grades: <50%, 50–69%, 70–99%, and complete occlusion. In the WASID trial, higher degrees of stenosis were associated with worse outcomes.⁵ Imaging techniques such as DSA, MRA, and CTA are commonly used to assess the degree of luminal stenosis (figure 1 and table 1). Additionally, transcranial Doppler may also provide estimations of arterial stenosis.⁶ While DSA, CTA, and MRA directly measure the lumen to determine stenosis, transcranial Doppler indirectly estimates stenosis by assessing blood flow velocity.^{2 7}

DSA provides detailed information about the anatomy, severity of the stenosis, and collateral circulation of the intracranial arteries. Its superior spatial resolution establishes DSA as the benchmark for luminal stenosis evaluation.^{4 8} Moreover, during DSA, endovascular procedures such as angioplasty

Table 1 Pros and cons of atherosclerotic plaque imaging modalities

	Pros	Cons	Luminal definition	Arterial wall and plaque	Spatial resolution	Hemodynamic information
DSA	<ul style="list-style-type: none"> ► Provides accurate visualization of the arterial lumen ► Interventions such as angioplasty and stenting can be performed during DSA ► Allows the assessment of real-time collaterals ► Can assess fractional flow reserve 	<ul style="list-style-type: none"> ► Invasive ► Luminal modality unable to assess plaque burden 	++++	+++	++++	++++
CTA	<ul style="list-style-type: none"> ► High sensitivity for plaque identification ► Calcifications can be visualized 	<ul style="list-style-type: none"> ► Less ideal for patients requiring follow-up imaging as it uses radiation 	+++	+++	++	+
MRA	<ul style="list-style-type: none"> ► Allows for visualization of luminal narrowing without radiation ► Various modalities such as time of flight (TOF) or contrast enhanced (CE) imaging can be used. TOF is less accurate than CE in assessing luminal stenosis 	<ul style="list-style-type: none"> ► Lower spatial resolution compared with DSA and CTA ► Arterial wall is not visualized unless it is accompanied by a HR-MRI protocol ► Contraindications to MRI, such as claustrophobia, not-MRI compatible pacemaker, among others 	+++	+	++	+
HR-MRI	<ul style="list-style-type: none"> ► Can visualize the arterial wall and plaque characteristics ► Identifies non-stenotic plaques with positive remodeling ► Does not use radiation 	<ul style="list-style-type: none"> ► Higher field of strength modalities such as 7T are not widely available ► Contraindications to MRI, such as claustrophobia, among others ► Very sensitive to movement artifact ► Long acquisition depending on the protocol 	+++	++++	+++	+
Transcranial US	<ul style="list-style-type: none"> ► Non-invasive ► Provides direct hemodynamic information about the degree of stenosis and possible collateral flow 	<ul style="list-style-type: none"> ► Cannot visualize the plaque directly ► Information is based on indirect measurements of blood velocity ► Operator dependent 	+	+	+	++
IVUS	<ul style="list-style-type: none"> ► Very high spatial resolution 	<ul style="list-style-type: none"> ► Invasive ► Neuro probes are not available 	+++	++++	++++	+
OCT	<ul style="list-style-type: none"> ► Highest spatial resolution with good correlation with cellular components 	<ul style="list-style-type: none"> ► Invasive ► Limited access to neuro probes 	++++	++++	++++	+

The accuracy of diagnostic ability is marked by the number of plus signs (+), from + (less accurate) to ++++ (most accurate).

CTA, CT angiography; DSA, digital subtraction angiography; HR-MRI, high resolution MRI; IVUS, intravenous ultrasound; MRA, MR angiography; OCT, optical coherence tomography.

or stenting can be performed and immediate intervention outcomes can be evaluated.⁹ An additional benefit of DSA is the potential to obtain flow hemodynamics by direct visualization of contrast opacification in the target vascular territory and collateral circulation, as well as through experimental approaches such as the use of a pressure guidewire for the measurement of fractional flow reserve (FFR).¹⁰ FFR is defined as the ratio of maximum flow in the presence of a stenosis to normal maximum flow.¹¹ FFR evaluates the influence of ICAD on cerebral vascular

dynamics, offering insights beyond what conventional stenosis measurements on DSA might reveal about downstream flow in the affected vascular territory.¹² However, despite DSA's detailed spatial resolution and hemodynamic data, it entails potential risks associated with the use of a catheter for intravascular access and selective injection of contrast. The rate of permanent neurological complications after DSA has been reported to be as high as 0.14%.¹³ The use of fluoroscopy exposes patients to cumulative radiation, particularly with multiple procedures.¹⁴ Moreover,

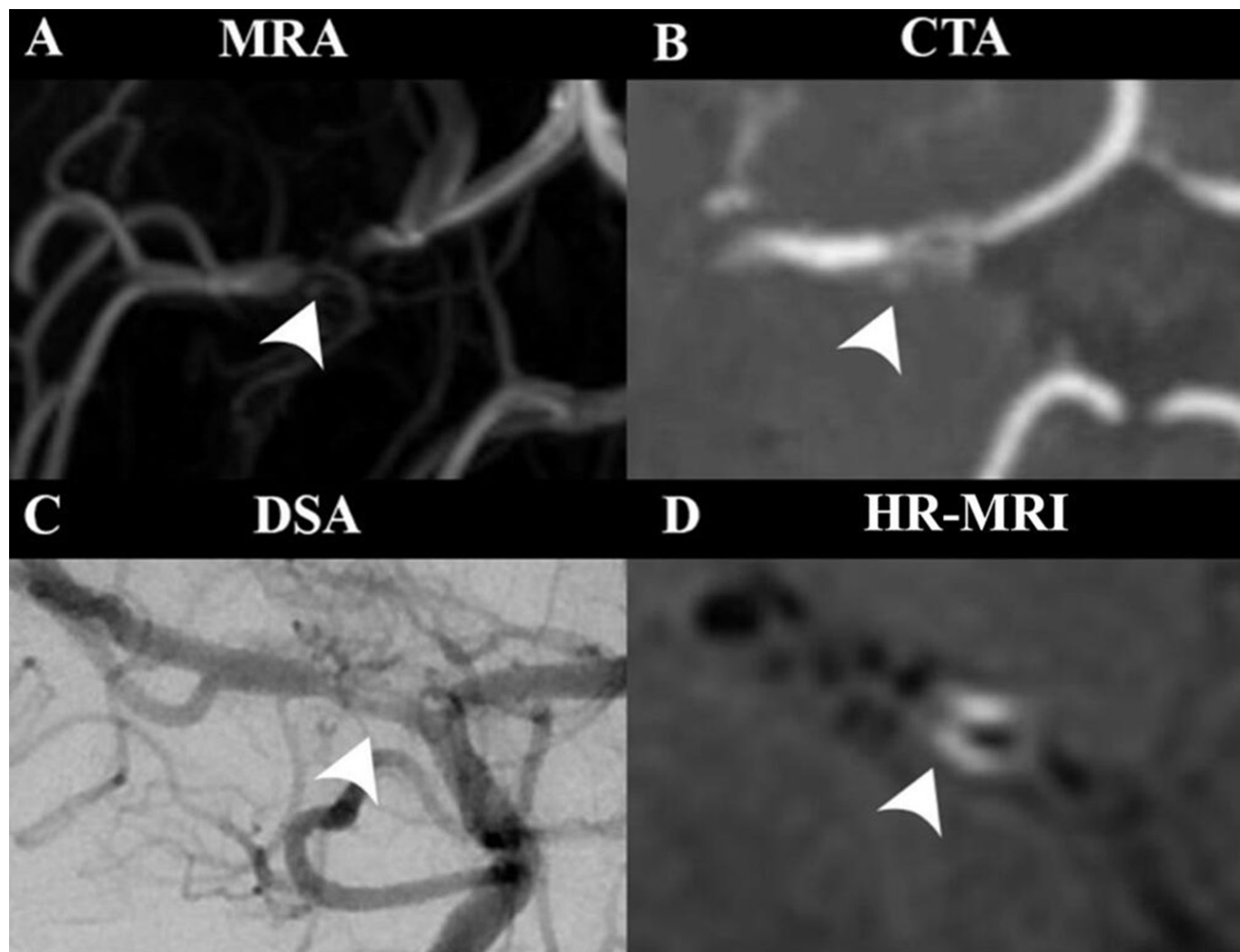


Figure 1 Imaging modalities for the assessment of intracranial atherosclerotic plaques. (A) Magnetic resonance angiography (MRA) shows a stenotic lesion (arrowhead) in the proximal segment of the middle cerebral artery (MCA). Nonetheless, it is not clear if the arterial segment is completely occluded or if there is a high-grade stenosis. (B) CT angiography (CTA) shows discontinuation of flow within the MCA (arrowhead). However, it is unclear if the affected arterial segment has an underlying plaque versus an area of dissection. (C) Digital subtraction angiography (DSA) shows a clear area of stenosis (arrowhead) with some neoangiogenesis. Based on the angiographic studies, it is unclear if the stenosis and Moyamoya-like neoangiogenesis is a primary Moyamoya disease versus a Moyamoya syndrome due to an advanced atherosclerotic process. (D) High-resolution MRI (HR-MRI) shows a heterogeneous gadolinium-enhancing plaque in the area of stenosis (arrowhead), suggesting that the neoangiogenesis is due to an advanced stenotic atherosclerotic process.

DSA is only a two-dimensional technique, and requires multiple projections to clearly define the degree of stenosis and the characteristics of an underlying plaque. In some instances such as acute mechanical thrombectomy, it is challenging to determine if the stenosis is caused by a plaque or a ‘fresh clot’.

CTA can visualize the arterial lumen and identify stenosis or occlusion. Nguyen-Huynh *et al* compared CTA and DSA in 41 patients with 275 pairs of intracranial arteries.¹⁵ CTA performed very well compared with DSA for detection of $\geq 50\%$ intracranial stenosis, achieving high sensitivity, specificity, and negative predictive values. The Stroke Outcomes and Neuroimaging of Intracranial Atherosclerosis (SONIA) study validated non-invasive imaging tests for ICAD against catheter angiography in a prospective and blinded multicenter setting.¹⁶ SONIA reported a positive predictive value of 13.3% and a negative predictive value of 83.8% for CTA when DSA defined stenosis as 70–99%.¹⁷ The study is more than 10 years from its publication and newer CT scans and post-processing techniques

have enhanced the accuracy of CTA on detecting stenosis when compared with DSA. Duffis *et al* performed a study involving 57 patients reporting a sensitivity of 96.6% and specificity of 99.4% for CTA in diagnosing stenosis $>50\%$ compared with DSA.¹⁸ New artificial intelligence (AI)-driven algorithms have tested the performance of CTA compared with DSA in detecting stenosis. Yang *et al* analyzed 296 patients who underwent CTA and DSA. The agreements for the detection of stenosis between the deep learning algorithm that analyzed CTA and DSA were good, with kappa values of 0.754, 0.695, 0.714, and 0.754 at the per-patient, per-region, per-arterial, and per-segment levels, respectively. Although the diagnostic performance was variable and modest at some levels, such as the segment level, it was high at the patient level for stenosis $\geq 50\%$ (sensitivity 0.895, specificity 0.938, area under the curve (AUC) 0.945).

CT perfusion (CTP) can also be used to identify areas of hypoperfusion due to the presence of ICAD. A study by de Havenon *et al* investigated the recurrence of symptomatic

ischemic stroke within 90 days in arterial territories exhibiting $\geq 50\%$ stenosis, as determined by perfusion imaging.¹⁹ Patients with hypoperfusion distal to the stenotic site had a higher likelihood of experiencing subsequent strokes in the same vascular territory (HR 6.80, 95% CI 2.31 to 20). It has been hypothesized that patients experiencing hemodynamic failure and possessing inadequate collateral circulation might benefit most from revascularization procedures. A post hoc analysis of the Stenting and Aggressive Medical Management for Preventing Recurrent stroke in Intracranial Stenosis (SAMMPRIS) trial reported that impaired collateral flow correlated with recurrent strokes in the territory of the affected artery.²⁰ Among those with watershed infarcts in the anterior circulation, 18.2% (10/55 patients) in the stenting group and 26.4% (14/53 patients) in the medical treatment group suffered a recurrent stroke, although this difference was not statistically significant ($P=0.30$). CTP may be used to determine the presence of collaterals and areas of downstream hypoperfusion.

MRA offers a non-invasive alternative for imaging, using techniques such as time-of-flight (TOF) MRA and contrast-enhanced (CE) MRA.^{21,22} However, MRA has lower spatial resolution than DSA and CTA. Bash *et al* studied 115 diseased arterial segments where CTA demonstrated higher sensitivity (98% vs 70%) and a positive predictive value (93% vs 65%) than TOF MRA for detecting intracranial stenosis.²³ It is important to note that, like DSA, MRA is a luminal modality and by itself cannot provide information about the arterial wall and may be susceptible to motion artifacts due to longer acquisition times,⁶ potentially affecting image quality and diagnostic accuracy. However, MRA has the advantage that a HR-MRI protocol including T2, T1 and T1 post Gd sequences can be performed during the same session and increase the detection and characterization of plaques. Furthermore, new methods that use deep learning algorithms may increase the diagnosis of stenosis in MRA. Qiu *et al* created a training set consisting of 291 lesions and used the information to test a set of 120 arterial segments. Their deep learning model achieved a sensitivity of 64.2% and a positive predictive value of 83.7% in detecting arterial stenosis in TOF MRA.²⁴ The performance of the algorithm decreased with moderate stenosis and smaller caliber arteries.

HR-MRI has progressively increased in use over the last 10 years, with more than 50% of members of the American Society of Neuroradiology performing this technique at their respective institutions. The most common application of HR-MRI is for vasculopathy differentiation (93.9%), ICAD characterization for symptomatic plaques (40.5%), and cryptogenic stroke assessment (40.9%).²⁵ ICAD has distinctive imaging characteristics on HR-MRI relative to other intracranial vasculopathies, specifically inflammatory vasculopathies, reversible cerebral vasoconstriction syndrome, and Moyamoya disease. On multi-contrast HR-MRI, ICAD typically appears as eccentric lesions, outwardly remodeled, that have heterogeneous, intermediate, or a significant degree of post-contrast enhancement, and have a juxta luminal T2-weighted hyperintense signal (fibrous cap) with a deeper hypointense signal (lipid-rich necrotic core).²⁶ Mossa-Basha *et al* performed a study with 21 patients to explore how HR-MRI performed compared with luminal modalities in the diagnosis of Moyamoya-like vascular changes. There was significant improvement in diagnostic accuracy with luminal imaging and HR-MRI when compared with luminal imaging alone (87% vs 32%, $P<0.001$). The most common arterial wall MRI findings for Moyamoya disease were non-enhancing, non-remodeling lesions without T2 heterogeneity. Atherosclerotic Moyamoya was characterized by eccentric remodeling, and T2

heterogeneous lesions with mild to moderate and homogeneous to heterogeneous contrast enhancement.²⁷ The same group later reported on the added benefit of HR-MRI in the differentiation between ICAD, vasculitis, and reversible vasoconstriction syndrome.²⁸ The likelihood of a correct diagnosis in the setting of non-occlusive vasculopathy significantly increased when HR-MRI was evaluated in addition to luminal imaging (per-lesion: 36.1–88.8%, per-patient: 43.5–96.3%). HR-MRI also excels in analyzing plaque composition and characterizing plaque types. An ex vivo study of 53 intracranial arteries demonstrated the high accuracy of 3T HR-MRI in identifying fibrolipid atheroma with a high interobserver agreement ($\kappa=0.77$).²⁹

Although not routinely used in clinical practice, higher field of strength scans have been used in the analysis of arterial atherosclerotic changes. 7T HR-MRI allows for more accurate visualization of plaque features than 3T HR-MRI.³⁰ Fakhri *et al* performed an analysis of 44 symptomatic patients with underlying ICAD who were imaged with DSA, CTA, and 7T HR-MRI. HR-MRI included TOF MRA, T1 and T1+Gd sequences, and was deemed as the gold standard in the characterization of atherosclerotic plaques with luminal stenosis and outward growth. When compared with 7T HR-MRI, DSA had a sensitivity of 88%, 3T TOF-MRA 78%, and CTA 76% in identifying symptomatic plaques.³¹ However, triage of patients for 7T HR-MRI is highly selective, and in this small cohort approximately 18% of patients had some contraindication to undergo a 7T-MRI. Other studies have confirmed that HR-MRI may surpass CTA in comparison to DSA in the evaluation of luminal stenosis. Liu *et al* conducted a comparative analysis between maximum intensity projection CTA and 3T HR-MRI to determine middle cerebral artery (MCA) stenosis against the gold standard DSA.³² They reported a stronger correlation between HR-MRI measurements and DSA, with a correlation coefficient of 0.68, in contrast to a coefficient of 0.45 for CTA. This underscores the accuracy of HR-MRI in the assessment of arterial stenosis.

HR-MRI also has the potential to characterize ICAD in patients with infarcts involving perforator arteries. While lacunar infarcts located in the basal nuclei, typically smaller than 1.5 cm, have been historically attributed to small arterial disease, HR-MRI has shown a notable burden of ICAD along the ventral and inferior walls of the MCA, challenging traditional notions that small infarcts in the deep basal nuclei are lacunar and not related to ICAD. In cases of symptomatic MCA stenosis, a significant number of plaques are also found in the superior wall, a hotspot for perforators ($P=0.001$).³³ A recent study by Meng *et al* analyzed 66 patients with symptomatic ICAD in the MCA who underwent endovascular treatment with percutaneous transluminal angioplasty.³⁴ All the patients who suffered periprocedural complications had plaques located in the superior wall of the MCA, suggesting that angioplasty led to a 'snow-plow' phenomenon in the perforators arising from the superior wall. Furthermore, research by Won *et al* indicates a higher frequency of perforating arteries associated with symptomatic plaques in the middle two-thirds of the M1 segment (41.4%).³⁵ Advanced imaging with 7T HR-MRI has identified key characteristics of symptomatic plaques such as the involvement of the origin of lenticulostriate arteries (OR 28.51, 95% CI 6.3 to 181) and plaque surface irregularity (OR 8.32, 95% CI 1.4 to 64.7), with plaques with greater wall thickness (1.36 mm) being more symptomatic. These findings may elucidate stroke mechanisms in patients with ICAD, distinguishing artery-to-artery thromboembolism from perforator strokes caused by plaque-induced occlusion at the origin of perforators. Recent studies suggest using submaximal angioplasty to conserve perforators

close to the stenotic lesion.³⁶ HR-MRI may identify symptomatic plaques not amenable for endovascular intervention due to possible compromise of perforators at the time of angioplasty, causing a ‘snow-plow’ effect. Similarly, the mid segment of the basilar artery, enriched with perforators, has been identified as a common site for atherosclerotic plaques that lead to ischemic strokes, and that pose an increased risk of complications at the time of endovascular angioplasty.³⁷

PLAQUE MORPHOLOGY BEYOND DEGREE OF STENOSIS

Luminal stenosis measurement has been a cornerstone for evaluating atherosclerotic plaque severity and has traditionally guided the inclusion criteria for numerous neurointerventional trials. These trials, such as the SAMMPRIS and the Vitesse Intracranial Stent Study for Ischemic Therapy (VISSIT), have required catheter angiography confirmation of 70–99% stenosis according to WASID criteria for patient selection.^{38,39} Recently, the China Angioplasty and Stenting for Symptomatic Intracranial Severe Stenosis (CASSISS) trial also implemented this strict luminal stenosis threshold to determine patient eligibility.⁴⁰ However, the inability of these trials to conclusively demonstrate the superiority of endovascular interventions might be attributed to a reliance on an overly simplistic assessment of symptomatic stenosis, primarily based on luminal narrowing, while not considering plaque morphology and composition (see online supplemental table 1). A further assessment with HR-MRI to determine the

PB instead of solely the degree of stenosis may aid in clinical decision making. This may be especially relevant in challenging scenarios such as non-stenotic atherosclerotic plaques. Trials using more detailed selection criteria, such as the Wingspan Stent System Post Market Surveillance (WEAVE) trial, have reported improved endovascular outcomes.⁴¹ In WEAVE, the criteria specified ICAD stenosis of 70–99% in arteries with a diameter of ≥ 2 mm. Submaximal angioplasty of 60% was applied to lesions near angiographically visible perforators. This approach significantly reduced the rate of periprocedural complications to 2.6%, a significant improvement over the 14.7% observed in the SAMMPRIS trial. Additionally, the incidence of periprocedural stroke attributed to perforator occlusion was markedly lower in WEAVE at 0.7%, compared with 5.8% in SAMMPRIS.

Newer high-resolution imaging techniques provide a better characterization of the PB in symptomatic patients. Studies have confirmed that the degree of stenosis alone may not fully capture the complexity and hemodynamic significance of intracranial atherosclerotic changes.^{42–44} Notably, certain features of atherosclerotic plaques are better observed through HR-MRI. PB, enhancement after contrast-Gd administration, and the presence of IPH have emerged as potential biomarkers of plaque instability (figure 2).^{31,44–46} Sometimes the use of HR-MRI has expanded the diagnosis of ICAD in patients previously classified as having cryptogenic stroke.⁴² Wang *et al* conducted a systematic review of 463 patients with acute ischemic stroke who did not have

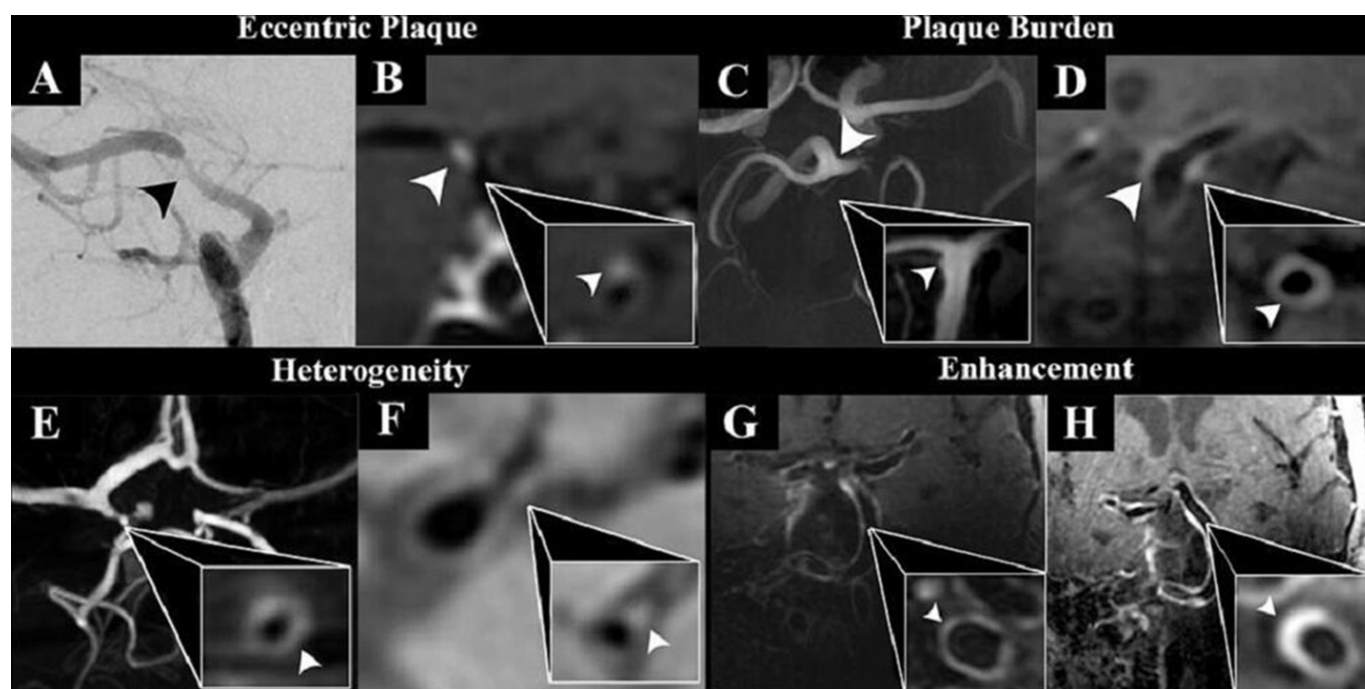


Figure 2 Characteristics of intracranial atherosclerotic plaques. Based on WASID criteria, the degree of stenosis caused by an atherosclerotic plaque is an important risk factor for stroke; however, other morphological characteristics of the plaque are also very relevant. (1) Eccentric versus concentric plaques. (A) This digital subtraction angiogram (DSA) shows a plaque (arrowhead) causing significant stenosis in the distal internal carotid artery (ICA). (B) A 7T high-resolution MRI (HR-MRI) shows the presence of an enhancing and eccentric plaque (arrowhead), suggesting that the most likely etiology of this stenosis is intracranial atherosclerosis. (2) Plaque burden. (C) In this case, magnetic resonance angiography (MRA) of a patient with cryptogenic stroke in the posterior circulation shows a small irregularity in the basilar artery (inset, arrowhead). (D) A 7T HR-MRI shows a circumferential plaque with significant plaque burden, despite no evident luminal stenosis (arrowhead) on MRA. (3) Heterogeneity. (E) The heterogeneity of the signal intensity within the plaque is possibly associated with intraplaque hemorrhage (IPH), the presence of calcification, or a lipid core. A 7T HR-MRI enables visualization of a heterogeneously enhancing plaque (arrowhead). (F) Moreover, hyperintense areas in T1-weighted images are suggestive of regions of angiogenesis and IPH within the plaque (arrowhead). (4) Enhancement. (G) A basilar artery plaque in a patient with recurrent transient ischemic attacks (arrowhead). (H) The patient did not start maximal medical therapy and the levels of low-density lipoprotein and HbA1c increased over time. Follow-up imaging showed increased plaque enhancement (arrowhead).

luminal stenosis on TOF MRA. In 50% of patients (233/463) an atherosclerotic plaque was identified with HR-MRI (95% CI 46.1% to 55.1%).⁴⁷

PB and plaque enhancement may be useful in discriminating between symptomatic and asymptomatic atherosclerotic plaques. A plaque is usually labeled as symptomatic if it is in the territory of the ischemic stroke.^{42–44} Two studies, one by Huang *et al* involving 91 plaques⁴⁸ and another by Sanchez *et al* who studied 80 plaques,⁴⁴ found that PB and enhancement after the administration of Gd were correlated with the presence of symptomatic plaques in patients with stroke symptoms due to ICAD. In contrast, the degree of luminal stenosis did not reliably identify symptomatic plaques. Both studies quantified PB and degree of stenosis through multiplanar measurements, which involved post-acquisition processing with selection of regions of interest (ROIs). Similarly, Shi *et al* analyzed 190 plaques with 3T HR-MRI and processed the signal intensity of T1 and T1+Gd sequences to generate histograms.⁴³ The distribution of signal intensity of atherosclerotic plaques was sampled with manually selected ROIs. IPH ($P=0.009$) and enhancement ratio in CE T1-weighted images ($P=0.006$) identified symptomatic and non-symptomatic plaques located in the basilar artery (BA). The authors divided stenosis into the following categories: <50%, 50–70%, >70%. Stenosis category was not associated with lesion type for either the MCA or BA as nearly 90% of symptomatic lesions had a degree of luminal stenosis of <70%. The study highlighted the potential benefit of a histogram-based analysis of signal intensity in the characterization of atherosclerotic plaques.

Because of their deep location and small size, it is hard to visualize and isolate the components of intracranial atherosclerotic plaques. Additionally, the thickness of the arterial walls within the circle of Willis may vary across both healthy and pathological segments, typically ranging from 0.45 to 0.66 mm.⁴⁹ This range is below the isotropic resolution recommended for intracranial vessel wall MRI by the Vessel Wall Imaging Study Group of the American Society of Neuroradiology.⁵⁰ A histogram-based analysis as described by Shi *et al*⁴³ may capture minor differences in the plaque morphology that are otherwise not apparent on conventional two-dimensional (2D) multiplanar views. The wider signal intensity dispersion in T1-weighted images suggests a heterogeneous composition within the arterial wall which may include lipids, IPH, calcium and fibrous tissue. IPH is especially relevant as it may be the result of the accumulation of blood within the plaque, maybe from the rupture of fragile neovascularized arteries within the unstable plaque.⁵¹ IPH is associated with local inflammation and progression of atherosclerosis. In proximal internal carotid disease, IPH was identified as areas within the plaque that have 150% higher signal intensity compared with the adjacent muscle.^{52–53} T1-weighted MR sequences are commonly used to detect IPH because the degradation of a hemorrhage produces methemoglobin, which results in T1 shortening and correspondingly causes high-signal intensity on T1-weighted MRI. Zhu *et al* performed a study using 3T HR-MRI on 122 BA atherosclerotic plaques and found that IPH was the strongest independent predictor of symptomatic status (OR 27.5).⁴⁶ IPH may also be a marker for stroke recurrence. Takaya *et al* imaged 154 subjects using 1.5T HR-MRI at baseline and followed them for an average of 38.2 months. Notably, the presence of IPH (HR 5.2; $P=0.005$) and a larger maximum wall thickness (HR for a 1 mm increase of 1.6; $P=0.008$) increased the risk of subsequent ischemic events.⁵⁴ Moreover, Zhu *et al* analyzed 22 BAs with IPH and noted that IPH can be present in both low-grade (<50%) and high-grade (>50%) stenotic BAs.⁴⁶ In our experience, the adjudication of IPH is challenging due

to the small size of atherosclerotic plaques (average thickness 1.4 mm), artifact introduced by movement and venous contamination, incomplete suppression of the cerebrospinal fluid and blood, and the subjectivity of the adjudicator.⁴⁴ Furthermore, hyperacute IPH may initially appear T1-isointense and transition to T1-hyperintensity during subacute and chronic stages.³

PB quantifies the amount of arterial remodeling or wall thickening in relation to the arterial lumen and is assessed by measuring the reduction in the cross-sectional area of the lumen at the site of the plaque compared with a reference arterial segment.⁵⁵ Plaques can remain non-stenotic despite having a high PB due to the outward thickening of the arterial wall. In other words, the arterial wall can undergo a process of outward growth without affecting the arterial lumen. This process is called 'positive remodeling' and has been correlated with the occlusion of small perforators and plaque instability. As discussed earlier, the occlusion of perforators is one of the main mechanisms in strokes caused by the presence of plaques in the superior wall of the MCA or the mid portion of the BA.^{33–37} Studies in coronary arteries have shown that plaques can grow up to 40% of PB without causing luminal stenosis.⁵⁶ Conversely, negative remodeling involves an inward thickening of the arterial wall.³¹ Two meta-analyses noted that positive remodeling was significantly associated with downstream ipsilateral stroke (OR 6.19 and OR 5.60).^{57–58} A higher PB is generally associated with an increased risk of plaque instability. Sanchez *et al* analyzed 36 patients imaged with 7T HR-MRI and reported that a higher PB was associated with the presence of symptomatic plaque in patients with multiple plaques (OR 6.1).⁴⁴ The mean PB for symptomatic plaques was 85 ± 13 and for non-symptomatic plaques was 65 ± 14 .⁴⁴ Monitoring changes in PB over time may provide valuable information regarding disease progression or response to medical therapy. In a study conducted by Sun *et al* involving 176 patients assessed with 3T HR-MRI, a 10% increase in PB correlated with a 2.4-fold increase in the OR for experiencing a recurrent stroke.⁵⁹ Another study using 3T HR-MRI observed that progression of PB was significantly associated with recurrent ischemic events (HR 6.29).⁶⁰ PB progression has also been correlated with the response to maximal medical therapy and the lipid profile. In a pilot study of five patients who were diagnosed with the presence of symptomatic atherosclerotic plaques and who received high-intensity statins, 7T HR-MRI demonstrated that PB decreased in parallel to decreased levels of low density lipoprotein at follow-up ($r=0.82$).⁶¹ Similarly, Guo *et al* analyzed 37 patients who underwent a 3T HR-MRI at baseline and at 1 year. The images were analyzed with the multitime point, multicontrast, and multiplanar viewing workflow called MOCHA. Longitudinal 3D intracranial arterial wall imaging showed that symptomatic plaques underwent luminal expansion. Interestingly, the presence of diabetes was associated with the progression of ICAD. Patients with diabetes had a 6.7% increase in wall thickness and a 6.6% decrease in lumen area at follow-up.⁶² Larger studies with 3T HR-MRI may confirm if maximal medical therapy can be tailored to morphological changes in the plaque and arterial wall.

Increased contrast-Gd uptake within the plaque results in higher enhancement and increased signal intensity in T1-weighted images. HR-MRI can be used to determine the amount of contrast enhancement of the plaque and the parent artery.^{42–44} Plaque enhancement has been correlated with increased inflammation and angiogenesis. As part of the process of atherosclerosis, neoangiogenesis can occur within the structure of the atherosclerotic artery. These fragile and leaky arteries can contribute to plaque enhancement. Millon *et al* studied 69 patients who

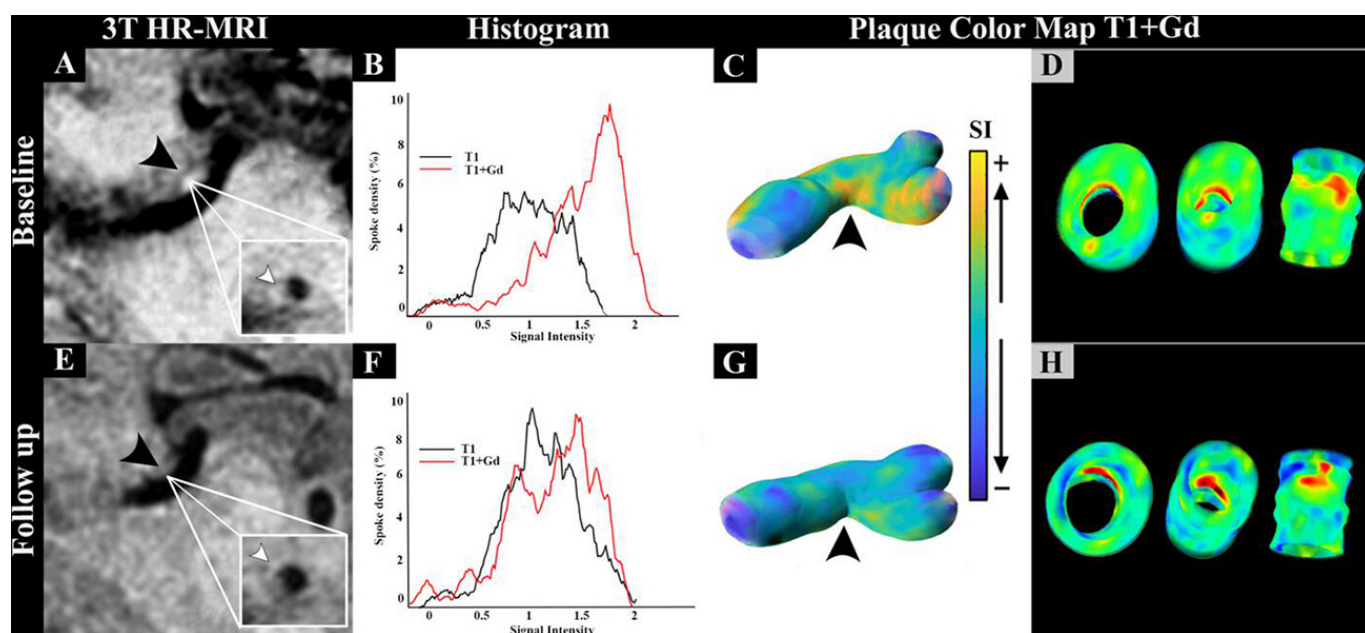


Figure 3 Three-dimensional plaque enhancement analysis. (A) An atherosclerotic plaque in the middle cerebral artery (black arrowhead). The plaque is enhanced with the administration of contrast gadolinium (Gd). This enhancement is visualized as high signal intensity. (B) On histogram analysis the first black curve represents the signal intensity in T1-weighted images. The second red curve shifts to the right as the signal intensity increases in T1-post Gd weighted images. (C, D) The increased Gd enhancement is visualized in 3D color maps. Color maps show high enhancement in areas of luminal stenosis (black arrowhead). (E) The same plaque is imaged at follow-up after initiation of maximal medical therapy (black arrowhead). The plaque enhancement has decreased significantly on visual assessment compared with the baseline plaque (white arrowhead). (F) On histogram analysis, the plaque barely captures contrast and the shift in the post-contrast curve is markedly reduced compared with the baseline histogram. (G, H) Plaque color maps show an objective change in enhancement at follow-up compared with baseline imaging. Areas of increased Gd enhancement (shown in yellow) have almost disappeared (black arrowhead).

underwent carotid endarterectomy and were imaged with 3T HR-MRI. Gd enhancement was observed in 59% of patients. Fibrous cap rupture ($P=0.043$), IPH ($P<0.0001$), and plaque enhancement ($P=0.034$) were significantly more frequent in symptomatic than in asymptomatic plaques. Histological analysis showed that Gd enhancement was significantly associated with the presence of vulnerable plaques (American Heart Association VI, $P=0.006$), neovascularization ($P<0.0001$), presence of macrophages ($P=0.030$), and loose fibrosis ($P<0.0001$). The prevalence of neoangiogenesis, macrophages, and loose fibrosis in the area of enhancement was 97%, 87%, and 80%, respectively.⁶³

Multiple meta-analyses have reported a significant association between plaque enhancement and the risk of downstream stroke (OR 10.8,⁶⁴ OR 10.09,⁵⁷ and OR 7.42⁵⁸), suggesting that plaques that enhance are more likely to rupture. Studies using 3T HR-MRI have also shown that higher enhancement ratios, which are measured by generating a ratio between the plaque enhancement in post-contrast and pre-contrast images, are more likely in patients with recurrent strokes compared with patients with only one ischemic event (OR 2.5).⁵⁹ Similarly, another prospective study that used 3T HR-MRI to follow 61 patients with ICAD during 56.3 ± 16.9 months observed that a post-contrast enhancement ratio of >1.77 was an independent predictor of future strokes.⁶⁵ Additionally, plaque enhancement could potentially be used in monitoring the response of plaques to medical therapies (figure 3). Chung *et al* performed 3T HR-MRI on 77 patients with ICAD who were treated with statins. At the follow-up assessment it was observed that statin therapy led to a significant reduction in the volume of plaque enhancement.⁶⁶ As mentioned earlier, a pilot study performed

by Sanchez *et al* with 7T HR-MRI on five patients with ICAD showed that comprehensive medical management including statins was associated with lower levels of low density lipoprotein cholesterol and reduced plaque enhancement at follow-up with a correlation coefficient of 0.8.⁶¹

OBJECTIVE QUANTIFICATION OF PLAQUE ENHANCEMENT WITH HR-MRI

Subjective quantification of atherosclerotic plaque enhancement remains a challenge due to various factors that can affect image quality. Incomplete cerebrospinal fluid and blood suppression can be mistaken as enhancement on post-contrast T1 images.⁶⁷ Furthermore, technical factors such as windowing and volume averaging may impact the accurate identification of enhancement.^{68,69} ‘Slow-flow artifact’ is another concern, where the vessel walls may appear artificially thickened due to insufficient suppression of the blood signal at the periphery, resulting from slow laminar flow.³ Additionally, the presence of the vasa vasorum along the proximal intracranial segments of the internal carotid artery (ICA) and the vertebral artery (VA) just beyond dural penetration may show mild enhancement, which can be mistakenly interpreted as enhancement of the vessel wall itself.⁶⁹ To overcome these limitations, quantitative methods for assessing enhancement have been developed (see online supplemental table 2). One such method is the enhancement ratio, which compares the signal intensity in the post-contrast T1-weighted image with the pre-contrast T1. This method can potentially differentiate between symptomatic and asymptomatic plaques.⁴³ Another approach calculates the contrast ratio between the plaque and the pituitary stalk. Huang *et al* performed 3T HR-MRI on 91 patients with ICAD and identified

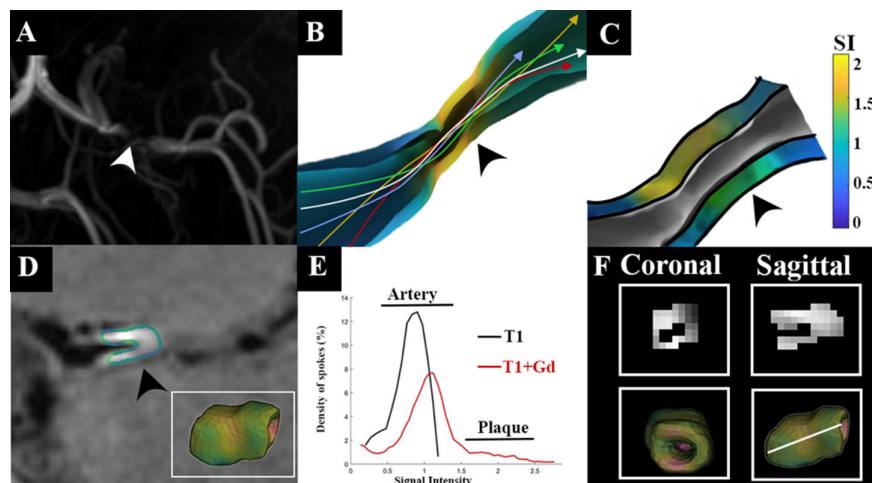


Figure 4 Imaging analysis method for evaluation of intracranial atherosclerotic plaques. (A) Magnetic resonance angiography provides a luminal view of a proximal middle cerebral artery atherosclerotic plaque causing significant stenosis (arrowhead). (B) Computational fluid dynamics simulates the flow through the stenotic area and can calculate the approximate shear forces through the area of stenosis (arrowhead). The stenosis leads to a transition from laminar flow to turbulent flow. (C) A three-dimensional (3D) analysis of the arterial wall (arrowhead) shows circumferential wall thickening (plaque burden) with inward stenosis. Areas of increased wall enhancement are shown in yellow. (D) The plaque is highly enhancing after the administration of contrast-gadolinium (Gd) (arrowhead), and the area of enhancement is clearly visualized in the 3D color map (inset). (E) First-order metrics such as histogram analysis can be derived from arterial wall mapping. In the depicted case, the histogram clearly indicates plaque enhancement following Gd administration, as evidenced by the tail of the histogram. (F) A voxel-based radiomic analysis can lead to the generation of second-order metrics based on the distribution of signal intensity. Emerging methods such as radiomics also facilitate the analysis of dimensional features of atherosclerotic plaques including volume, size, and diameter.

that a contrast ratio stalk of 0.56 or more had a sensitivity of 68.3% and a specificity of 81.8% in identifying symptomatic plaques.⁴⁸ Similarly, Fakih *et al* used 7T HR-MRI to study plaque enhancement with a contrast ratio stalk. A threshold of 0.53 had a sensitivity of 78% and a specificity of 62% for symptomatic plaque detection.⁴²

While previous methods focused on 2D multiplanar measurements, recent advancements have introduced 3D analysis techniques (figure 4). Sanchez *et al* developed a post-acquisition processing method to generate 3D color maps of arterial and plaque enhancement, with dozens of orthogonal probes projecting into the plaque to sample its signal intensity. On average, 125 ± 79 data points per plaque and 858 ± 564 per arterial segment are obtained through this post-acquisition method. In this 7T HR-MRI study, 3D color maps generated from the analysis of Gd uptake were the most accurate metric for identifying symptomatic plaques (OR 3.9). A multivariate model combining 3D Gd uptake and PB demonstrated 83% sensitivity and 86% specificity for identifying symptomatic plaques in patients with various plaques. Moreover, 3D Gd enhancement was more sensitive (86% vs 70%) and specific (71% vs 68%) in identifying symptomatic plaques than conventional 2D measurements. This 3D method also allows for a comprehensive assessment of plaque signal intensity, potentially allowing for a detailed analysis of the plaque components. For instance, atherosclerotic plaques with IPH had a higher SD on the histogram generated through 3D mapping,⁴⁴ suggesting that plaques with IPH have a more heterogeneous distribution of signal intensity and therefore achieve higher SD.

Recently, radiomics has emerged as a new tool for assessing atherosclerotic plaques by extracting multiple variables from single voxels. Unlike traditional methods that rely solely on raw signal intensity values, radiomics provides a comprehensive analysis that explores various features. It quantifies histogram-based values, textural values that capture the interaction of individual

voxels, and shape-based features.⁷⁰ Radiomics analysis has been previously used with great success in oncology by estimating cell heterogeneity and characteristics, and ultimately improving diagnostic accuracy.⁷¹ Recently, there has been a growing body of evidence supporting the application of radiomics in the imaging of ICAD, indicating its potential to improve the understanding and management of this condition. In a study by Shi *et al*, a radiomics-based analysis was performed on 96 patients who underwent 3T HR-MRI. The study incorporated established high-risk characteristics such as minimal luminal area, presence of IPH, and Gd enhancement. Additionally, the authors developed a radiomic model based on these features. The performance of the radiomic model was superior to the traditional model, with an AUC of 0.93 compared with 0.83. When the two models were combined, an even higher performance was achieved with an AUC of 0.97.⁷² This study suggests that radiomics has the potential to provide a comprehensive assessment of atherosclerotic plaques. Although radiomics holds great potential in the characterization of atherosclerotic plaques, there is still a need for a correlation between specific radiomic features and histological findings.

HEMODYNAMIC ANALYSIS OF INTRACRANIAL ATHEROSCLEROTIC PLAQUES

Computational fluid dynamics (CFD) offers insights into the interactions between blood flow and arterial walls. One of the key measurements obtained from CFD is Wall Shear Stress (WSS), which quantifies the tangential force exerted by blood flow on the arterial wall (figure 4).⁷³ WSS is further defined by time-averaged Wall Shear Stress (TAWSS) and the Wall Shear Stress Gradient (WSSG). TAWSS reflects the average changes in WSS across cardiac cycles,⁷⁴ and WSSG quantifies the magnitude of changes in the WSS along blood vessels. Additionally, the Oscillatory Shear Index assesses variations in WSS vector magnitude throughout the cycle.⁷⁵ Under normal physiological

conditions, a minimal gradient of shear stress is exerted by blood flow on the inner vessel wall.⁷⁶ Research suggests that low WSS may contribute to the development of arterial plaques, often occurring at points of arterial bifurcation or in regions where blood recirculation is common.⁷⁷⁻⁷⁸ Chen *et al* conducted a comparative study between 94 MCA plaques in patients with atherosclerosis and 50 normal MCAs, and found that low WSS was prevalent in plaque-affected areas.⁷⁹ Low WSS may increase endothelial cell turnover and lipid accumulation, particularly in areas with erratic flow. This is partly attributed to the expansion of gap junctions between endothelial cells, which may facilitate the uptake and deposition of lipids, promoting plaque formation.⁸⁰⁻⁸²

CFD analysis may shed light on the morphological transformations within atherosclerotic plaques post-formation. Symptomatic plaques are often characterized by a large lipid core beneath a delicate fibrous cap. The rupture of this cap leads to platelet adhesion and subsequent thrombus formation, a process that significantly contributes to the onset of ischemic strokes.³⁸⁻⁸³ Huang *et al* investigated 35 patients with BA plaques with ruptured fibrous caps.⁸⁴ The presence of a ruptured fibrous cap correlated with increased WSS proximal to arterial stenosis compared with those without ruptured fibrous caps. This suggests a potential link between WSS and plaque vulnerability. Furthermore, Woo *et al* examined 110 patients to explore the relationship between WSS distribution and stroke.⁸⁵ They discovered that patients at risk of artery-to-artery embolism often had localized high WSS, which may precipitate plaque instability and subsequent rupture, underscoring the importance of WSS as a potential factor in distinct stroke mechanisms.

WSS patterns can change with the regression of intracranial stenosis. This may occur when plaques remodel in response to optimal medical therapy. Lan *et al* studied 39 patients with ICAD who underwent a CTA at baseline and at 1-year follow-up. Lesions with a higher maximum WSS and a larger high-WSS area were more likely to have regression of luminal stenosis at follow-up after maximal medical therapy. Higher focal WSS may improve along with decreased stenosis under appropriate medical therapy.⁸⁶ While WSS offers valuable insights into the fluid dynamics of atherosclerosis, it is crucial to acknowledge the multifactorial nature of fluid mechanics.⁸⁷ For instance, factors such as age, blood pressure, and body mass index may alter WSS.⁸⁸ Additionally, conducting CFD analysis demands substantial technical proficiency and has not yet become universally adopted.

Phase-contrast quantitative MRA (QMRA) has been used to assess arterial blood flow within the vertebrobasilar (VB) system, providing insights into collateral flow and the hemodynamic consequences of luminal stenosis.⁸⁹ In the VERITAS study, Amin-Hanjani *et al* examined patients who had experienced a recent VB transient ischemic attack or stroke and had at least 50% atherosclerotic stenosis or occlusion in the VB system.⁹⁰ Flow measurement using QMRA suggested that patients with reduced distal flow faced a significantly increased risk of subsequent stroke if they had symptomatic atherosclerotic VB disease (HR 11.5, 95% CI 1.8 to 17; $P=0.008$). Shakur *et al* studied 44 patients with carotid stenosis using the post-processing tool derived from QMRA known as Noninvasive Optimal Arterial Analysis software (NOVA). In their study, a higher percentage stenosis and smaller residual lumen were associated with a significant decrease in ICA flow.⁹¹ Additionally, it was observed that the mean MCA flow ratio between the affected and unaffected sides was significantly reduced in patients exhibiting symptoms as opposed to those without symptoms.

INTRALUMINAL IMAGING OF ATHEROSCLEROTIC PLAQUES

IVUS involves the insertion of a catheter-mounted ultrasound probe into the blood vessel of interest, providing real-time, high-resolution images of the arterial lumen and the underlying arterial wall.⁹² IVUS provides detailed information about the characteristics of atherosclerotic plaques. Nair *et al* imaged 88 ex-vivo coronary plaques and found a high correlation between IVUS radiofrequency analysis and histopathological findings.⁹³ IVUS enables the assessment of plaque morphology, including plaque eccentricity, ulceration, and remodeling. It can visualize the size, shape, and surface characteristics of the plaque, aiding in the understanding of plaque stability and the risk of plaque rupture. Dabus *et al* used IVUS to determine the formation of pseudoaneurysms in patients with ICAD who underwent intracranial stenting.⁹⁴ IVUS clearly defined the presence of ulcerations on large plaques that had positive remodeling and that looked on luminal DSA as new aneurysms. Although IVUS is a potential imaging technique, it remains an invasive procedure and its use in the intracranial arteries has been limited to case series.⁹⁵⁻⁹⁶

OCT is an alternative to IVUS. Although OCT has lower tissue penetration compared with IVUS (1–3 mm vs 4–8 mm),⁹² it provides higher resolution (1–15 μm vs 100 μm).⁹⁷ OCT can add great value in determining the morphological characteristics of the arterial wall (figure 5).⁹⁸ Shi *et al* correlated OCT with the presence of macrophages on histological analysis. Ex vivo OCT images were co-registered with histopathology in 282 cross-sectional pairs from 19 carotid endarterectomy specimens. Subsequently, they performed clinical analysis of 93 patients who were analyzed with OCT and then analyzed the burden of macrophage infiltration. Using the OCT data and histological analysis, the authors generated an algorithm that had a sensitivity of 88% and a specificity of 74.9% for detecting macrophage infiltration. OCT showed that macrophage infiltration was much more predominant in ruptured plaques than in non-ruptured plaques (83.7% vs 32.0%, $P<0.001$).⁹⁸ Similarly, Yabushita *et al* correlated 357 atherosclerotic arterial OCT images with their histological analysis obtained at autopsy. Calcific nodules were identified with OCT with 96% sensitivity and 97% specificity. Finally, in a comparative analysis, Jang *et al* examined 42 coronary plaques to assess the diagnostic capabilities of OCT versus IVUS in plaque characterization. OCT was more effective than IVUS in identifying features such as intimal hyperplasia and echolucent regions, potentially indicative of lipid pools.⁹⁹ Autopsy studies have shown that OCT can identify plaques with >10% macrophage density within the fibrous cap and with microchannels representing neovascularization.¹⁰⁰ OCT has great clinical potential in identifying atherosclerotic lesions due to its higher spatial resolution compared with HR-MRI.¹⁰¹ Similar to IVUS, OCT is an invasive imaging technique with the potential risk of complications, including arterial dissection.¹⁰² Developments in high-frequency OCT technology are ongoing, with the creation of newer and softer OCT probes that are expected to enhance the intraluminal characterization of atherosclerosis in the foreseeable future.¹⁰³

FUNCTIONAL IMAGING OF ATHEROSCLEROSIS THROUGH POSITRON EMISSION TOMOGRAPHY

The previously described imaging methods focus solely on evaluating plaque morphology, yet they do not completely quantify functional aspects of atherosclerotic plaque formation. This is a multifaceted process involving inflammation, macrophage accumulation, lipid deposition, and smooth muscle migration.¹⁰⁴ Positron emission tomography (PET) employs positron-emitting

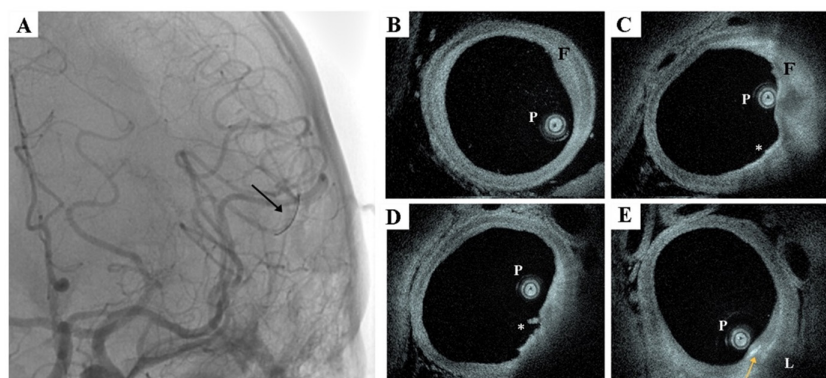


Figure 5 High-frequency neuro-optical coherence tomography (nOCT, Spryte Medical) in a cadaver. (A) The 0.014 inch probe was delivered to the M3 division of the left middle cerebral artery (arrow) via an 0.021 inch microcatheter from a femoral artery approach. Although angiography did not demonstrate significant luminal narrowing, extensive intracranial atherosclerotic disease was present. (B–E) nOCT images (B,3 distal to proximal, respectively, of the M1 trunk) suggest various characteristics of atherosclerotic disease such as intimal thickening with a fibrotic plaque (F in B and C), an area of macrophage infiltration (asterisk in C), plaque erosion (asterisk in D), cholesterol crystal (arrow in E), and lipid accumulation (L in E).

radioligands such as ^{18}F -fluorodeoxyglucose (FDG) that can accumulate at these biological processes. This accumulation results in a concentrated emission of positrons, which promptly interact with electrons in nearby tissues, leading to biochemical reactions. These reactions generate gamma photons that are detectable by the PET scanner.¹⁰⁵ Rudd *et al* imaged eight patients with symptomatic carotid atherosclerosis using ^{18}F -FDG-PET. Six of these patients had bilateral carotid plaques and two had normal contralateral arteries. Symptomatic carotid plaques were visible in the FDG-PET images acquired 3 hours after FDG injection. The estimated net FDG accumulation rate in symptomatic lesions was 27% higher than in contralateral asymptomatic lesions. Interestingly, no measurable FDG uptake was observed in carotid arteries without plaque.¹⁰⁶ Similarly, Liu *et al* conducted a study analyzing 13 histological specimens using PET. They found that regions with high FDG uptake were significantly more likely to contain inflammatory cells ($P < 0.001$) and neovasculature ($P = 0.008$) compared with regions with low FDG uptake. Additionally, areas with complex inflammatory cell infiltrate, characterized by co-localized macrophages, lymphocytes, and foam cells, showed the highest FDG uptake among inflammatory subgroups ($P < 0.001$).¹⁰⁷ PET has also been used in the assessment of non-stenotic plaques. Davies *et al* imaged 12 patients with symptomatic carotid disease using FDG-PET and HR-MRI. Interestingly, three patients had non-stenotic lesions identified on HR-MRI that had a high level of FDG uptake. All three of the highly inflamed non-stenotic lesions were located in a vascular territory compatible with the patients' presenting symptoms.¹⁰⁸ Finally, PET has the potential to evaluate neoangiogenesis in the setting of ICAD. A recent study by Shu *et al* used Ga-NOTA-PRGD2, a marker that binds to activated endothelial cells, to evaluate angiogenesis in patients with ICAD. Ga-NOTA-PRGD2 uptake in the peri-infarct, subcortical, and periventricular regions of the symptomatic side was higher than the contralateral hemisphere ($P = 0.001$).¹⁰⁹

CONCLUSION

Evaluating ICAD solely by the degree of luminal stenosis fails to capture the complexity of atherosclerotic changes within cerebral arteries. Advanced imaging techniques such as HR-MRI offer a more nuanced assessment, identifying specific plaque characteristics linked to a higher risk of symptomatic ICAD. These characteristics include PB, IPH, and post-Gd plaque enhancement—markers associated with active inflammation

and symptomatic plaques. Such detailed features are beyond the reach of traditional luminal imaging like CTA, MRA, and DSA. Enhanced post-processing methods, including 3D enhancement mapping and radiomic analysis, are pioneering new metrics for ICAD evaluation and monitoring the efficacy of medical treatments. These require clinical validation to ensure their utility and accuracy in clinical practice. Physiological metrics such as CFD analysis and QMRA further characterize hemodynamic plaque characteristics, providing insights beyond mere stenotic measurements. OCT, despite being an invasive method with restricted availability, stands out for its unparalleled spatial resolution among imaging modalities, offering an exceptionally detailed view of plaque morphology. PET is a promising research tool as it can potentially identify inflammatory markers within the plaque. These advanced technologies promise to refine our understanding and treatment of ICAD, moving beyond traditional models to a more comprehensive and tailored approach.

X Edgar A Samaniego @esamaniego

Contributors SS, MMB, VA, DSL: Data collection and manuscript drafting. EAS: Conception and design, drafting and revising the article.

Funding This work was conducted on an MRI instrument founded by (1S10OD0250225-01) at the University of Iowa.

Competing interests None declared.

Patient consent for publication Not applicable.

Ethics approval Not applicable.

Provenance and peer review Commissioned; externally peer reviewed.

Supplemental material This content has been supplied by the author(s). It has not been vetted by BMJ Publishing Group Limited (BMJ) and may not have been peer-reviewed. Any opinions or recommendations discussed are solely those of the author(s) and are not endorsed by BMJ. BMJ disclaims all liability and responsibility arising from any reliance placed on the content. Where the content includes any translated material, BMJ does not warrant the accuracy and reliability of the translations (including but not limited to local regulations, clinical guidelines, terminology, drug names and drug dosages), and is not responsible for any error and/or omissions arising from translation and adaptation or otherwise.

ORCID iDs

Sebastian Sanchez <http://orcid.org/0009-0000-3696-8361>
Mahmud Mossa-Basha <http://orcid.org/0000-0001-7798-8158>
Vania Anagnostakou <http://orcid.org/0000-0001-5101-3192>
Edgar A Samaniego <http://orcid.org/0000-0003-2764-2268>

REFERENCES

- Holmstedt CA, Turan TN, Chimowitz MI. Atherosclerotic intracranial arterial stenosis: risk factors, diagnosis, and treatment. *Lancet Neurol* 2013;12:1106–14.

- 2 Chen LH, Spagnolo-Allende A, Yang D, *et al.* Epidemiology, pathophysiology, and imaging of atherosclerotic intracranial disease. *Stroke* 2024;55:311–23.
- 3 Kang D-W, Kim DY, Kim J, *et al.* Emerging concept of intracranial arterial diseases: the role of high resolution vessel wall MRI. *J Stroke* 2024;26:26–40.
- 4 Samuels OB, Joseph GJ, Lynn MJ, *et al.* A standardized method for measuring intracranial arterial stenosis. *AJNR Am J Neuroradiol* 2000;21:643–6.
- 5 Chimowitz MI, Kokkinos J, Strong J, *et al.* The warfarin-aspirin symptomatic intracranial disease study. *Neurology* 1995;45:1488–93.
- 6 Charles JH, Desai S, Jean Paul A, *et al.* Multimodal imaging approach for the diagnosis of intracranial atherosclerotic disease (ICAD): basic principles, current and future perspectives. *Interv Neuroradiol* 2024;30:105–19.
- 7 Robba C, Goffi A, Geeraerts T, *et al.* Brain ultrasonography: methodology, basic and advanced principles and clinical applications. A narrative review. *Intensive Care Med* 2019;45:913–27.
- 8 Hill MD, Demchuk AM, Frayne R. Noninvasive imaging is improving but digital subtraction angiography remains the gold standard. *Neurology* 2007;68:2057–8.
- 9 Almallouhi E, de Havenon A, Asi K, *et al.* RESCUE-ICAS: rationale and study design. *SVIN* 2023;3:e000530.
- 10 Zanaty M, Rossen JD, Roa JA, *et al.* Intracranial atherosclerosis: a disease of functional, not anatomic stenosis? How trans-stenotic pressure gradients can help guide treatment. *Oper Neurosurg (Hagerstown)* 2020;18:599–605.
- 11 Pu Y, Lan L, Leng X, *et al.* Intracranial atherosclerosis: from anatomy to pathophysiology. *Int J Stroke* 2017;12:236–45.
- 12 Yang P, Wan S, Wang J, *et al.* Hemodynamic assessment for intracranial atherosclerosis from angiographic images: a clinical validation study. *J Neurointerv Surg* 2024;16:204–8.
- 13 Kaufmann TJ, Huston J III, Mandrekar JN, *et al.* Complications of diagnostic cerebral angiography: evaluation of 19,826 consecutive patients. *Radiology* 2007;243:812–9.
- 14 Willinsky RA, Taylor SM, TerBrugge K, *et al.* Neurologic complications of cerebral angiography: prospective analysis of 2,899 procedures and review of the literature. *Radiology* 2003;227:522–8.
- 15 Nguyen-Huynh MN, Wintermark M, English J, *et al.* How accurate is CT angiography in evaluating intracranial atherosclerotic disease? *Stroke* 2008;39:1184–8.
- 16 Feldmann E, Wilterdink JL, Kosinski A, *et al.* The Stroke Outcomes and Neuroimaging of Intracranial Atherosclerosis (SONIA) trial. *Neurology* 2007;68:2099–106.
- 17 Liebeskind DS, Kosinski AS, Saver JL, *et al.* Computed tomography angiography in the Stroke Outcomes and Neuroimaging of Intracranial Atherosclerosis (SONIA) study. *Interv Neurol* 2014;2:153–9.
- 18 Duffis EJ, Jethwa P, Gupta G, *et al.* Accuracy of computed tomographic angiography compared to digital subtraction angiography in the diagnosis of intracranial stenosis and its impact on clinical decision-making. *J Stroke Cerebrovasc Dis* 2013;22:1013–7.
- 19 de Havenon A, Khatri P, Prabhakaran S, *et al.* Hypoperfusion distal to anterior circulation intracranial atherosclerosis is associated with recurrent stroke. *J Neuroimaging* 2020;30:468–70.
- 20 Wabnitz AM, Derdeyn CP, Fiorella DJ, *et al.* Hemodynamic markers in the anterior circulation as predictors of recurrent stroke in patients with intracranial stenosis. *Stroke* 2019;50:143–7.
- 21 Kiruluta AJM, González RG. Magnetic resonance angiography: physical principles and applications. *Handb Clin Neurol* 2016;135:B978-0-444-53485-9.00007-6:137–49.
- 22 Schaafsma JD, Silver FL, Kasner SE, *et al.* Infarct patterns in patients with atherosclerotic vertebrobasilar disease in relation to hemodynamics. *Cerebrovasc Dis Extra* 2019;9:123–8.
- 23 Bash S, Villablanca JP, Jahan R, *et al.* Intracranial vascular stenosis and occlusive disease: evaluation with CT angiography, MR angiography, and digital subtraction angiography. *AJNR Am J Neuroradiol* 2005;26:1012–21.
- 24 Qiu J, Tan G, Lin Y, *et al.* Automated detection of intracranial artery stenosis and occlusion in magnetic resonance angiography: a preliminary study based on deep learning. *Magnetic Resonance Imaging* 2022;94:105–11.
- 25 Mossa-Basha M, Zhu C, Yuan C, *et al.* Survey of the American Society of Neuroradiology membership on the use and value of intracranial vessel wall MRI. *AJNR Am J Neuroradiol* 2022;43:951–7.
- 26 Mossa-Basha M, Hwang WD, De Havenon A, *et al.* Multicontrast high-resolution vessel wall magnetic resonance imaging and its value in differentiating intracranial vasculopathic processes. *Stroke* 2015;46:1567–73.
- 27 Mossa-Basha M, de Havenon A, Becker KJ, *et al.* Added value of vessel wall magnetic resonance imaging in the differentiation of Moyamoya vasculopathies in a non-Asian cohort. *Stroke* 2016;47:1782–8.
- 28 Mossa-Basha M, Shibata DK, Hallam DK, *et al.* Added value of vessel wall magnetic resonance imaging for differentiation of nonocclusive intracranial vasculopathies. *Stroke* 2017;48:3026–33.
- 29 Jiang Y, Zhu C, Peng W, *et al.* Ex-vivo imaging and plaque type classification of intracranial atherosclerotic plaque using high resolution MRI. *Atherosclerosis* 2016;249:10–6.
- 30 Anumula S, Song HK, Wright AC, *et al.* High-resolution black-blood MRI of the carotid vessel wall using phased-array coils at 1.5 and 3 Tesla. *Acad Radiol* 2005;12:1521–6.
- 31 Fakhri R, Varon Miller A, Raghuram A, *et al.* High resolution 7T MR imaging in characterizing culprit intracranial atherosclerotic plaques. *Interv Neuroradiol* 2022;2022:15910199221145760.
- 32 Liu Q, Huang J, Degnan AJ, *et al.* Comparison of high-resolution MRI with CT angiography and digital subtraction angiography for the evaluation of middle cerebral artery atherosclerotic steno-occlusive disease. *Int J Cardiovasc Imaging* 2013;29:1491–8.
- 33 Xu W-H, Li M-L, Gao S, *et al.* Plaque distribution of stenotic middle cerebral artery and its clinical relevance. *Stroke* 2011;42:2957–9.
- 34 Meng Y, Magigi MC, Song Y, *et al.* Plaque features of the middle cerebral artery are associated with periprocedural complications of intracranial angioplasty and stenting. *Neuroradiology* 2024;66:109–16.
- 35 Won SY, Cha J, Choi HS, *et al.* High-resolution intracranial vessel wall MRI findings among different middle cerebral artery territory infarction types. *Korean J Radiol* 2022;23:333–42.
- 36 Alexander MJ, Yu W. Intracranial atherosclerosis update for neurointerventionalists. *J Neurointerv Surg* 2024;16:522–8.
- 37 Samaniego EA, Shaban A, Ortega-Gutierrez S, *et al.* Stroke mechanisms and outcomes of isolated symptomatic basilar artery stenosis. *Stroke Vasc Neurol* 2019;4:189–97.
- 38 Chimowitz MI, Lynn MJ, Turan TN, *et al.* Design of the stenting and aggressive medical management for preventing recurrent stroke in intracranial stenosis trial. *J Stroke Cerebrovasc Dis* 2011;20:357–68.
- 39 Zaidat OO, Fitzsimmons B-F, Woodward BK, *et al.* Effect of a balloon-expandable intracranial stent vs medical therapy on risk of stroke in patients with symptomatic intracranial stenosis: the VISSIT randomized clinical trial. *JAMA* 2015;313:1240–8.
- 40 Gao P, Wang T, Wang D, *et al.* Effect of stenting plus medical therapy vs medical therapy alone on risk of stroke and death in patients with symptomatic intracranial stenosis: the CASSISS randomized clinical trial. *JAMA* 2022;328:534–42.
- 41 Alexander MJ, Zauner A, Chaloupka JC, *et al.* WEAVE trial: final results in 152 on-label patients. *Stroke* 2019;50:889–94.
- 42 Fakhri R, Roa JA, Bathla G, *et al.* Detection and quantification of symptomatic atherosclerotic plaques with high-resolution imaging in cryptogenic stroke. *Stroke* 2020;51:3623–31.
- 43 Shi Z, Li J, Zhao M, *et al.* Quantitative histogram analysis on intracranial atherosclerotic plaques. *Stroke* 2020;51:2161–9.
- 44 Sanchez S, Raghuram A, Fakhri R, *et al.* 3D enhancement color maps in the characterization of intracranial atherosclerotic plaques. *AJNR Am J Neuroradiol* 2022;43:1252–8.
- 45 Shi Z, Hu B, Schoepf UJ, *et al.* Artificial intelligence in the management of intracranial aneurysms: current status and future perspectives. *AJNR Am J Neuroradiol* 2020;41:373–9.
- 46 Zhu C, Tian X, Degnan AJ, *et al.* Clinical significance of Intraplaque hemorrhage in low- and high-grade basilar artery stenosis on high-resolution MRI. *AJNR Am J Neuroradiol* 2018;39:1286–92.
- 47 Wang Y, Liu X, Wu X, *et al.* Culprit intracranial plaque without substantial stenosis in acute ischemic stroke on vessel wall MRI: a systematic review. *Atherosclerosis* 2019;287:112–21.
- 48 Huang L-X, Wu X-B, Liu Y-A, *et al.* Qualitative and quantitative plaque enhancement on high-resolution vessel wall imaging predicts symptomatic intracranial atherosclerotic stenosis. *Brain Behav* 2023;13:e3032.
- 49 Harteveld AA, Denswil NP, Van Hecke W, *et al.* Ex vivo vessel wall thickness measurements of the human circle of Willis using 7T MRI. *Atherosclerosis* 2018;273:106–14.
- 50 Mandell DM, Mossa-Basha M, Qiao Y, *et al.* Intracranial vessel wall MRI: principles and expert consensus recommendations of the American Society of Neuroradiology. *AJNR Am J Neuroradiol* 2017;38:218–29.
- 51 Mura M, Della Schiava N, Long A, *et al.* Carotid intraplaque haemorrhage: pathogenesis, histological classification, imaging methods and clinical value. *Ann Transl Med* 2020;8:1273.
- 52 Altaf N, Daniels L, Morgan PS, *et al.* Detection of Intraplaque hemorrhage by magnetic resonance imaging in symptomatic patients with mild to moderate carotid stenosis predicts recurrent neurological events. *J Vasc Surg* 2008;47:337–42.
- 53 Yu JH, Kwak HS, Chung GH, *et al.* Association of intraplaque hemorrhage and acute infarction in patients with basilar artery plaque. *Stroke* 2015;46:2768–72.
- 54 Takaya N, Yuan C, Chu B, *et al.* Association between carotid plaque characteristics and subsequent ischemic cerebrovascular events: a prospective assessment with MRI-initial results. *Stroke* 2006;37:818–23.
- 55 Teng Z, Peng W, Zhan Q, *et al.* An assessment on the incremental value of high-resolution magnetic resonance imaging to identify culprit plaques in atherosclerotic disease of the middle cerebral artery. *Eur Radiol* 2016;26:2206–14.
- 56 Fishbein MC, Siegel RJ. How big are coronary atherosclerotic plaques that rupture? *Circulation* 1996;94:2662–6.
- 57 Lee HN, Ryu CW, Yun SJ. Vessel-wall magnetic resonance imaging of intracranial atherosclerotic plaque and ischemic stroke: a systematic review and meta-analysis. *Front Neurol* 2018;9:1032.
- 58 Song JW, Pavlou A, Xiao J, *et al.* Vessel wall magnetic resonance imaging biomarkers of symptomatic intracranial atherosclerosis. *Stroke* 2021;52:193–202.

- 59 Sun B, Wang L, Li X, *et al.* Intracranial atherosclerotic plaque characteristics and burden associated with recurrent acute stroke: a 3D quantitative vessel wall MRI study. *Front Aging Neurosci* 2021;13:706544.
- 60 Shi Z, Li J, Zhao M, *et al.* Progression of plaque burden of intracranial atherosclerotic plaque predicts recurrent stroke/transient ischemic attack: a pilot follow-up study using higher-resolution MRI. *J Magn Reson Imaging* 2021;54:560–70.
- 61 Sanchez S, Miller JM, Jones MT, *et al.* Intracranial atherosclerotic plaque morphologic pattern and enhancement change with high-intensity statin therapy. *SVIN* 2023;3:e000942.
- 62 Guo Y, Canton G, Baylam Geler D, *et al.* Plaque evolution and vessel wall remodeling of intracranial arteries: a prospective, longitudinal vessel wall MRI study. *J Magn Reson Imaging* 2024.
- 63 Millon A, Boussel L, Brevet M, *et al.* Clinical and histological significance of gadolinium enhancement in carotid atherosclerotic plaque. *Stroke* 2012;43:3023–8.
- 64 Gupta A, Baradaran H, Al-Dasuqi K, *et al.* Gadolinium enhancement in intracranial atherosclerotic plaque and ischemic stroke: a systematic review and meta-analysis. *J Am Heart Assoc* 2016;5:e003816.
- 65 Gómez-Vicente B, Hernández-Pérez M, Martínez-Velasco E, *et al.* Intracranial atherosclerotic plaque enhancement and long-term risk of future strokes: a prospective, longitudinal study. *J Neuroimaging* 2023;33:289–301.
- 66 Chung J-W, Cha J, Lee MJ, *et al.* Intensive statin treatment in acute ischaemic stroke patients with intracranial atherosclerosis: a high-resolution magnetic resonance imaging study (STAMINA-MRI study). *J Neurol Neurosurg Psychiatry* 2020;91:204–11.
- 67 Cornelissen BMW, Leemans EL, Coolen BF, *et al.* Insufficient slow-flow suppression mimicking aneurysm wall enhancement in magnetic resonance vessel wall imaging: a phantom study. *Neurosurg Focus* 2019;47:E19.
- 68 Song JW, Wasserman BA. Vessel wall MR imaging of intracranial atherosclerosis. *Cardiovasc Diagn Ther* 2020;10:982–93.
- 69 Kang N, Qiao Y, Wasserman BA. Essentials for interpreting intracranial vessel wall MRI results: state of the art. *Radiology* 2021;300:492–505.
- 70 van Griethuysen JJM, Fedorov A, Parmar C, *et al.* Computational radiomics system to decode the radiographic phenotype. *Cancer Res* 2017;77:e104–7.
- 71 Wang X, Xie T, Luo J, *et al.* Radiomics predicts the prognosis of patients with locally advanced breast cancer by reflecting the heterogeneity of tumor cells and the tumor microenvironment. *Breast Cancer Res* 2022;24:20.
- 72 Shi Z, Zhu C, Degnan AJ, *et al.* Identification of high-risk plaque features in intracranial atherosclerosis: initial experience using a radiomic approach. *Eur Radiol* 2018;28:3912–21.
- 73 Hartman EMJ, De Nisco G, Gijzen FJH, *et al.* The definition of low wall shear stress and its effect on plaque progression estimation in human coronary arteries. *Sci Rep* 2021;11:22086.
- 74 Migliori S, Chiastra C, Bologna M, *et al.* Application of an OCT-based 3D reconstruction framework to the hemodynamic assessment of an ulcerated coronary artery plaque. *Med Eng Phys* 2020;78:74–81.
- 75 Ku DN, Giddens DP, Zarins CK, *et al.* Pulsatile flow and atherosclerosis in the human carotid bifurcation. Positive correlation between plaque location and low oscillating shear stress. *Arteriosclerosis* 1985;5:293–302.
- 76 Dolan JM, Kolega J, Meng H. High wall shear stress and spatial gradients in vascular pathology: a review. *Ann Biomed Eng* 2013;41:1411–27.
- 77 Zhou M, Yu Y, Chen R, *et al.* Wall shear stress and its role in atherosclerosis. *Front Cardiovasc Med* 2023;10:1083547.
- 78 Kumar N, Pai R, Abdul Khader SM, *et al.* Influence of blood pressure and rheology on oscillatory shear index and wall shear stress in the carotid artery. *J Braz Soc Mech Sci Eng* 2022;44.
- 79 Chen Y, Liu J, Li M, *et al.* Non-invasive assessment of intracranial wall shear stress using high-resolution magnetic resonance imaging in combination with computational fluid dynamics technique. *Fundamental Research* 2022;2:329–34.
- 80 Dhawan SS, Avati Nanjundappa RP, Branch JR, *et al.* Shear stress and plaque development. *Expert Rev Cardiovasc Ther* 2010;8:545–56.
- 81 Meng H, Tutino VM, Xiang J, *et al.* High WSS or low WSS? Complex interactions of hemodynamics with intracranial aneurysm initiation, growth, and rupture: toward a unifying hypothesis. *AJNR Am J Neuroradiol* 2014;35:1254–62.
- 82 Raghuram A, Galloy A, Nino M, *et al.* Comprehensive morphomechanical analysis of brain aneurysms. *Acta Neurochir (Wien)* 2023;165:461–70.
- 83 Yuan C, Zhang S, Polissar NL, *et al.* Identification of fibrous cap rupture with magnetic resonance imaging is highly associated with recent transient ischemic attack or stroke. *Circulation* 2002;105:181–5.
- 84 Huang R, Chen H, Li C, *et al.* Increased proximal wall shear stress of basilar artery plaques associated with ruptured fibrous cap. *Brain Sci* 2022;12:1397.
- 85 Woo HG, Kim H-G, Lee KM, *et al.* Wall shear stress associated with stroke occurrence and mechanisms in middle cerebral artery atherosclerosis. *J Stroke* 2023;25:132–40.
- 86 Lan L, Liu H, Ip V, *et al.* Regional high wall shear stress associated with stenosis regression in symptomatic intracranial atherosclerotic disease. *Stroke* 2020;51:3064–73.
- 87 Li Z-Y, Taviani V, Tang T, *et al.* The mechanical triggers of plaque rupture: shear stress vs pressure gradient. *Br J Radiol* 2009;82 Spec No 1:S39–45.
- 88 Shaaban AM, Duerinckx AJ. Wall shear stress and early atherosclerosis: a review. *AJR Am J Roentgenol* 2000;174:1657–65.
- 89 Amin-Hanjani S, Du X, Zhao M, *et al.* Use of quantitative magnetic resonance angiography to stratify stroke risk in symptomatic vertebrobasilar disease. *Stroke* 2005;36:1140–5.
- 90 Amin-Hanjani S, Pandey DK, Rose-Finnell L, *et al.* Effect of hemodynamics on stroke risk in symptomatic atherosclerotic vertebrobasilar occlusive disease. *JAMA Neurol* 2016;73:178.
- 91 Shakur SF, Hrbac T, Alaraj A, *et al.* Effects of extracranial carotid stenosis on intracranial blood flow. *Stroke* 2014;45:3427–9.
- 92 Pavlin-Premrl D, Sharma R, Campbell BCV, *et al.* Advanced imaging of intracranial atherosclerosis: lessons from interventional cardiology. *Front Neurol* 2017;8:387.
- 93 Nair A, Kuban BD, Tuzcu EM, *et al.* Coronary plaque classification with Intravascular ultrasound radiofrequency data analysis. *Circulation* 2002;106:2200–6.
- 94 Dabus G, Linfante I, Samaniego EA. De novo pseudoaneurysm formation after angioplasty and stenting of posterior circulation intracranial atherosclerotic disease: mechanism, characterization with intravascular ultrasound and management considerations. *J Neurointerv Surg* 2013;5:447–51.
- 95 Takayama K, Taoka T, Nakagawa H, *et al.* Successful percutaneous transluminal angioplasty and stenting for symptomatic intracranial vertebral artery stenosis using Intravascular ultrasound virtual histology. *Radiat Med* 2007;25:243–6.
- 96 Wehman JC, Holmes DR, Hanel RA, *et al.* Intravascular ultrasound for intracranial angioplasty and stent placement: technical case report. *Neurosurgery* 2006;59:SE481–3.
- 97 Li Y, Chen J, Chen Z. Multimodal Intravascular imaging technology for characterization of atherosclerosis. *J Innov Opt Health Sci* 2020;13.
- 98 Shi X, Tao T, Wang Y, *et al.* Heavy macrophage infiltration identified by optical coherence tomography relates to plaque rupture. *Ann Clin Transl Neurol* 2023;10:2334–46.
- 99 Jang I-K, Bouma BE, Kang D-H, *et al.* Visualization of coronary atherosclerotic plaques in patients using optical coherence tomography: comparison with Intravascular ultrasound. *J Am Coll Cardiol* 2002;39:604–9.
- 100 Abtahian F, Jang IK. Optical coherence tomography: basics, current application and future potential. *Curr Opin Pharmacol* 2012;12:583–91.
- 101 Anagnostakou V, Ughi GJ, Puri AS, *et al.* Optical coherence tomography for neurovascular disorders. *Neuroscience* 2021;474:134–44.
- 102 Barbieri L, D'Errico A, Avallone C, *et al.* Optical coherence tomography and coronary dissection: precious tool or useless surplus. *Front Cardiovasc Med* 2022;9:822998.
- 103 Anagnostakou V, Epshtein M, Ughi GJ, *et al.* Transvascular in vivo microscopy of the subarachnoid space. *J Neurointerv Surg* 2022;14:420–8.
- 104 Bäck M, Yurdagül A Jr, Tabas I, *et al.* Inflammation and its resolution in atherosclerosis: mediators and therapeutic opportunities. *Nat Rev Cardiol* 2019;16:389–406.
- 105 Evans NR, Tarkin JM, Chowdhury MM, *et al.* PET imaging of atherosclerotic disease: advancing plaque assessment from anatomy to pathophysiology. *Curr Atheroscler Rep* 2016;18:30.
- 106 Rudd JHF, Warburton EA, Fryer TD, *et al.* Imaging atherosclerotic plaque inflammation with [¹⁸F]-fluorodeoxyglucose positron emission tomography. *Circulation* 2002;105:2708–11.
- 107 Liu J, Kerwin WS, Caldwell JH, *et al.* High resolution FDG-microPET of carotid atherosclerosis: plaque components underlying enhanced FDG uptake. *Int J Cardiovasc Imaging* 2016;32:145–52.
- 108 Davies JR, Rudd JHF, Fryer TD, *et al.* Identification of culprit lesions after transient ischemic attack by combined 18F fluorodeoxyglucose positron-emission tomography and high-resolution magnetic resonance imaging. *Stroke* 2005;36:2642–7.
- 109 Shu S, Zhang L, Zhu YC, *et al.* Imaging angiogenesis using (68)Ga-NOTA-PRGD2 positron emission tomography/computed tomography in patients with severe intracranial atherosclerotic disease. *J Cereb Blood Flow Metab* 2017;37:3401–8.

Comprehensive Imaging Analysis of Intracranial Atherosclerosis

Sebastian Sanchez,¹ Mahmud Mossa-Basha,² Vania Anagnostakou,³ David S Liebeskind,⁴ and Edgar A Samaniego⁵

1. Yale University, Department of Neurology, New Haven, USA
2. University of Washington, Department of Radiology, Seattle, USA
3. University of Massachusetts, Department of Radiology, Amherst, USA
4. University of California at Los Angeles, Department of Neurology, Los Angeles, USA
5. University of Iowa, Departments of Neurology, Neurosurgery and Radiology, Iowa City, USA

Supplementary material

Tables

Supplementary table 1. Features of Symptomatic Plaques

Imaging Technique	Stenosis	PB	IPH	Positive Remodeling	Fibrous cap	Gd Enhancement
DSA	++++	-	-	-	-	-
CTA	+++	+	-	+	+	-
MRA	+++	+	-	+	-	+
HR-MRI	+++	++++	++++	++++	+++	++++
Transcranial US	++	-	-	-	-	-
IVUS	+++	+++	++++	++	++++	-
OCT	+++	++++	++++	++++	++++	-

The accuracy of diagnostic capability is denoted by the number of plus signs, ranging from "+" for the least accurate to "++++" for the most accurate. PB: plaque burden. PB: plaque burden. DSA: Digital subtraction angiography. CTA: Computated tomography angiography. MRA: Magnetic resonance angiography. HR-MRI: High resolution mangnetic resonance imaging. Transcranial US: Transcranial ultrasound. IVUS: Intravascular ultrasound. OCT: Optic coherence tomography. IPH: Intraplaque hemorrhage. Gd: Gadolinium.

Supplementary table 2. Method for quantification of Plaque Enhancement.

Author	Method	MRI	Metric	Finding
Kim et al(1)	Expert adjudication	3T	Presence of Enhancement	Plaque enhancement was independently associated with stroke recurrence (HR: 7.42, 95% CI 1.74–31.75, p = 0.007).
Qiao et al(2)	Expert adjudication	3T	Enhancement grade	Grade 2 enhancement, adjusted for plaque thickness, was associated with symptomatic plaques (OR 34.6; 95% CI 4.5, 266.5) compared with grade 0. Grade 0 was only present in asymptomatic plaques.
Shi et al (3)	Objective 2D	3T	Histogram-derived coefficient of variation	Coefficient of variation was an independent predictor for symptomatic plaques in both the MCA and BA with a sensitivity of 79% and a specificity of 80%
Shi et al(4)	Objective 2D	3T	Enhancement ratio	Enhancement ratio was independently associated with acute/subacute symptoms. The enhancement ratio for acute/subacute symptomatic plaques was 24.20 ± 29.46 while for asymptomatic plaques was 3.38 ± 21.91 p <0.001
Shi et al (4)	Objective 2D	3T	Radiomics	A model that included plaque radiomic features from T1 and T1+Gd images had a sensitivity of 97.0% and specificity of 79.0% for acute/sub-acute symptomatic plaques
Huang et al(5)	Objective 2D	3T	CR Stalk	CR Stalk ≥ 0.56 had a sensitivity of 68.3% and a specificity of 81.8% for identifying symptomatic plaques
Fakih et al (6)	Objective 2D	7T	CR Stalk	CR Stalk ≥ 0.53 had a sensitivity of 78% and a specificity of 62% for identifying symptomatic plaques
Sanchez et al(7)	Objective 3D	7T	3D Gd-uptake	3D Gd uptake of ≥ 1.23 had a sensitivity of 86% versus and specificity of 71% for symptomatic plaques

The presence of enhancement after the administration of contrast-Gd has been determined with different approaches. Kim et al adjudicated enhancement subjectively on visual assessment as present or absent.(1) Qiao et al used an enhancement scale, grade 0 = enhancement less than normal arterial walls, grade 1 = enhancement higher than grade 0 but lower than the pituitary stalk, and grade 2 = enhancement greater than or equal to that of the pituitary stalk.(2) Shi et al generated histograms from the coefficient of variation derived from signal intensity change. The coefficient of variation was calculated as the signal intensity standard deviation/ mean signal intensity.(3) Shi et al used radiomics for determining enhancement. This post-acquisition

processing method yields multiple features based on a voxel-derived histogram, textural, and shape analysis.(4) Shi et al also used the enhancement ratio which can be quantified as : $((\text{signal of plaque [post-contrast]}/\text{signal of grey matter [post-contrast]}) / (\text{signal of plaque [pre-contrast]}/\text{signal of grey matter [pre-contrast]}) - 1) \times 100\%$. Other investigators such as Huang et al and Fakhri et al, have used the pituitary stalk ratio (CR stalk) for determining the amount of enhancement. CR stalk is measured using the following formula: $\text{Signal intensity of the plaque in T1+Gd} / \text{Signal intensity of the pituitary stalk in T1+Gd}$.(6) 3D Gd uptake is quantified as: $(\text{mean of the Plaque T1+Gd} - \text{mean of the Plaque T1}) / \text{Standard deviation of the plaque in T1}$.(7)

References

1. Kim J-M, Jung K-H, Sohn C-H, Moon J, Shin J-H, Park J, et al. Intracranial plaque enhancement from high resolution vessel wall magnetic resonance imaging predicts stroke recurrence. *International Journal of Stroke*. 2016;11(2):171-9.
2. Qiao Y, Zeiler SR, Mirbagheri S, Leigh R, Urrutia V, Wityk R, et al. Intracranial Plaque Enhancement in Patients with Cerebrovascular Events on High-Spatial-Resolution MR Images. *Radiology*. 2014;271(2):534-42.
3. Shi Z, Li J, Zhao M, Peng W, Meddings Z, Jiang T, et al. Quantitative Histogram Analysis on Intracranial Atherosclerotic Plaques. *Stroke*. 2020;51(7):2161-9.
4. Shi Z, Zhu C, Degnan AJ, Tian X, Li J, Chen L, et al. Identification of high-risk plaque features in intracranial atherosclerosis: initial experience using a radiomic approach. *Eur Radiol*. 2018;28(9):3912-21.
5. Huang LX, Wu XB, Liu YA, Guo X, Ye JS, Cai WQ, et al. Qualitative and quantitative plaque enhancement on high-resolution vessel wall imaging predicts symptomatic intracranial atherosclerotic stenosis. *Brain Behav*. 2023:e3032.
6. Fakhri R, Roa JA, Bathla G, Olalde H, Varon A, Ortega-Gutierrez S, et al. Detection and Quantification of Symptomatic Atherosclerotic Plaques With High-Resolution Imaging in Cryptogenic Stroke. *Stroke*. 2020;51(12):3623-31.
7. Sanchez S, Raghuram A, Fakhri R, Wendt L, Bathla G, Hickerson M, et al. 3D Enhancement Color Maps in the Characterization of Intracranial Atherosclerotic Plaques. *American Journal of Neuroradiology*. 2022.